Geophysical Journal International

Geophys. J. Int. (2012) **190,** 1657–1672 doi: 10.1111/j.1365-246X.2012.05570.x

The south of Java earthquake of 1921 September 11: a negative search for a large interplate thrust event at the Java Trench

Emile A. Okal

Department Earth and Planetary Sciences, Northwestern University, Evanston, IL 60208, *USA. E-mail: emile@earth.northwestern.edu*

Accepted 2012 June 8. Received 2012 June 5; in original form 2012 March 30

SUMMARY

We present a detailed study of the earthquake of 1921 September 11, located between the two anomalous 'tsunami earthquakes' of 1994 and 2006 south of Java. Based on modern relocation techniques, a compilation of focal mechanism constraints from historical seismograms, a quantification of mantle surface waves, and a numerical simulation of its mediocre tsunami (only 10 cm at Cilacap), we conclude that the 1921 earthquake occurred at a depth of 30 km, as an intraplate earthquake in the outer rise, featuring a mostly strike-slip mechanism expressing tensional stress parallel to the direction of convergence, with a moment of 5×10^{27} dyn cm.

Two other large historical earthquakes south of Java (in 1937 and 1943) are also shown to be intraplate shocks, so that the Java subduction zone lacks large interplate thrust events for the entire era of instrumental seismicity. However, this does not violate the extrapolation to large sources of the frequency-moment characteristics of modern digital data (1976–2011), thus leaving open the possibility that the Java trench might entertain occasional, if rare, mega-thrust events.

Key words: Tsunamis; Earthquake source observations; Subduction zone processes; Indian Ocean.

GJI Seismology

1 INTRODUCTION AND BACKGROUND

This paper addresses the question of the possible existence of large interplate thrust earthquakes in a subduction zone—the Java Trench—where two 'tsunami earthquakes' occurred on 1994 June 2 and 2006 July 17. Our study of three large historical events (in 1921, 1937 and 1943) concludes that none of them was an interplate thrust.

We recall that the concept of 'tsunami earthquakes', introduced by Kanamori (1972), characterizes events whose tsunami is significantly larger than expected from their seismic magnitudes, especially conventional ones. Their source spectrum is deficient in high frequencies which makes them treacherous as they are not felt to their real potential by local populations, who find themselves deprived of any natural warning before an often catastrophic tsunami is unleashed onto the nearby coastlines. This tragic scenario occurred in Java in 1994 and 2006 (Tsuji *et al.* 1995; Fritz *et al.* 2007).

In very general terms, tsunami earthquakes take place under two frameworks: in the first one, described by Fukao (1979), they occur as aftershocks of regular megathrust events, triggered by stress transfer from the main shock into a medium featuring deficient mechanical properties (hence slower rupture), such as an accretionary wedge on the overlying plate. Examples include the tsunami earthquakes of 1963 October 20 and 1975 June 10 in the Kuril Islands (Fukao 1979), and 1932 June 22 in Mexico (Okal & Borrero 2011). In the second framework, described by Tanioka *et al.* (1997), tsunami earthquakes occur as individual shocks, whose rupture takes place along the uppermost part of the plate interface, characterized either by irregular contacts in sediment-starved environments (Polet & Kanamori 2000), or by the existence of a zone of reduced rigidity along the interplate contact, itself resulting from the ingestion, compaction and dehydration of sediments along its uppermost part (Bilek & Lay 1999; Lay & Bilek 2007). Examples of this scenario include the 1946 Unimak, 1947 Hikurangi, 1992 Nicaragua, 1996 Chimbote, Peru, 1994 and 2006 Java events. The Mentawai earthquake of 2010 October 25 (Newman *et al.* 2011) would fit the geometry of the second framework even though it could be regarded as an aftershock of the larger 2007 Bengkulu event. As for the 1896 Meiji Sanriku earthquake, it may fall under the first one, but with a continuous rupture where the aftershock occurs without time delay (Tanioka & Satake 1996).

Under the second framework, an intriguing question regarding tsunami earthquakes is whether their presence along a subduction zone precludes the occurrence of mega-thrust events of potentially larger size, but with more regular strain release. The absence of known megathrust events in Nicaragua, northern Peru and at the Hikurangi Trough would support the concept, while the occurrence of the 2011 Tohoku megathrust event along the same subduction system as the 1896 tsunami earthquake would oppose it.

Among such systems figures the Java Trench, where the oceanic lithosphere of the Australian plate, aged 125 Ma, subducts under the Sunda block of the Eurasian plate (Mueller *et al.* 1997). The full convergence rate between Australia and Borneo is estimated at

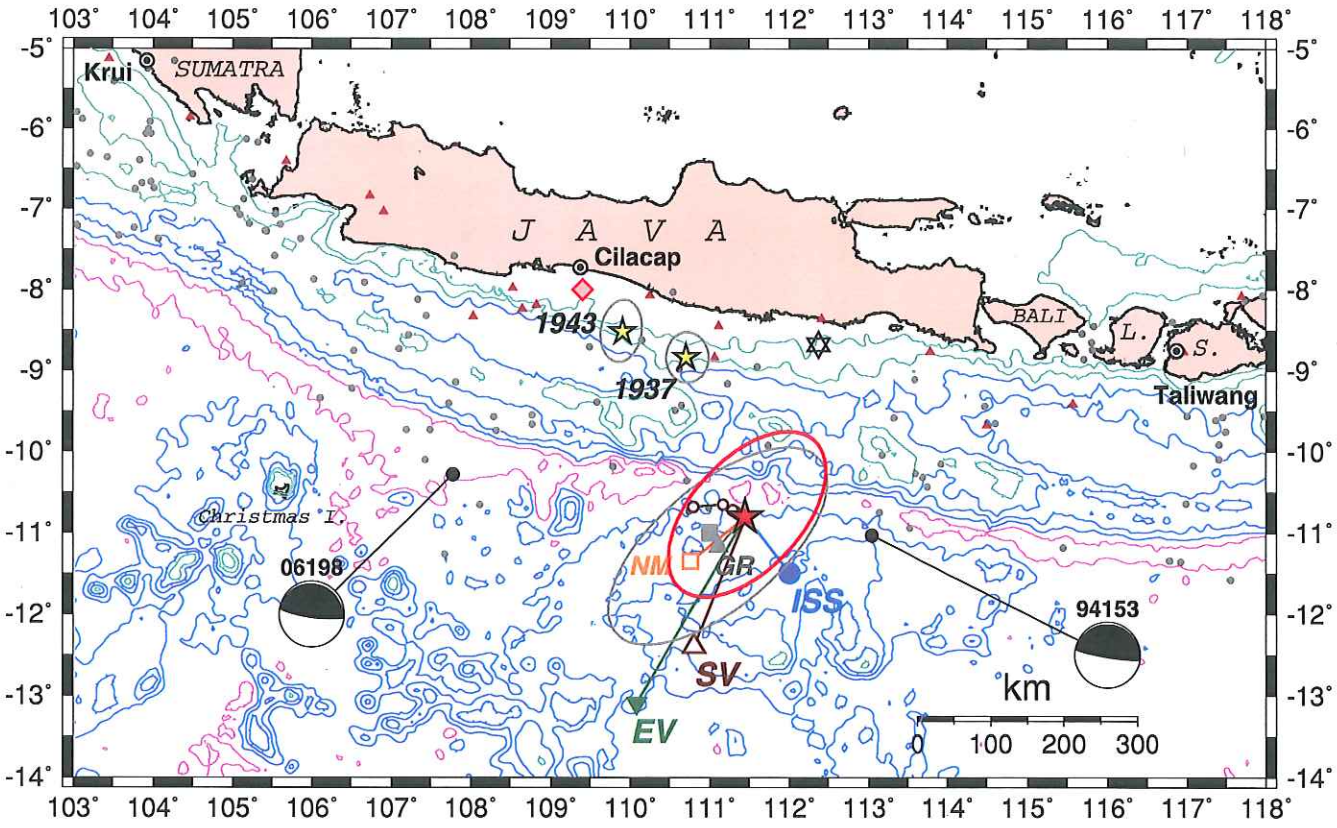

Figure 1. Relocation of the 1921 earthquake. The preferred relocation is shown as the red star, with associated confidence ellipse. The grey square denotes Gutenberg & Richter's (1954) original location (GR), with the triangle showing our relocation of B. Gutenberg's data set (with confidence ellipse). The blue circle shows the ISS location, the orange open square Newcomb & McCann's (1987) relocation (NM), and the green inverted triangle the Centennial catalogue epicentre (EV). The brown open triangle (SV) is Visser's (1922) epicentral estimate. The small chain of open circles to the west of the star represents the moveout of the relocated epicentre upon changing the depth. The small symbols show the background seismicity, as defined from the Global CMT catalogue (grey dots: $h < 70$ km; brown triangles: $70 < h < 200$ km). The star of David shows the location of a seaquake report by the *S.S. Salawatti*. The two tsunami earthquakes of 1994 and 2006 are shown with their associated focal mechanisms. Isobaths are shown at 1000-m intervals (1000 and 2000 m: green; 3000 to 5000 m: blue; 6000 and 7000 m: purple). The smaller stars to the north of the 1921 event are the two relocated events of 1937 and 1943. The diamond offshore Cilacap shows the location of the virtual gauge used in the tsunami simulations.

7.7 cm yr^{-1} (Sella *et al.* 2002). Under Ruff & Kanamori's (1980) model, such tectonic parameters would suggest a maximum moment of 6×10^{27} dyn cm for interplate thrust earthquakes, a figure essentially identical to the 1994 and 2006 values (5.3 and 4. 6×10^{27} dyn cm, respectively), which could then represent the upper limit of expectable interplate thrust events at the Java Trench. We note however that Ruff & Kanamori's (1980) model was disproved by the 2004 Sumatra and more recently 2011 Tohoku earthquakes, and that consequently, a cautionary approach now earmarks all sufficiently long subduction zones as potential hosts of megathrust events (Stein & Okal 2007; McCaffrey 2007).

Background seismicity in the Java Trench (106–119°E) exhibits an intriguing quiescence in terms of interplate thrust events. Over the available lifetime of the GlobalCMT catalogue (presently spanning 1976 January to 2011 November), and with the exception of the two tsunami earthquakes of 1994 and 2006, the largest event identifiable as an interplate thrust occurred south of Sumba on 1977 January with a moment of only 3.1×10^{25} dyn cm. All larger earthquakes either have a substantially different geometry, or occurred in the over-riding plate, e.g. under Bali or Flores Islands. The question of the possible existence, at the Java Trench, of events of potentially much greater size is crucially important to the assessment of tsunami risk, not only in Indonesia, but also along the nearby western coast of Australia, which hosts economically vital infrastructure, and even, in the far field, in the Mascarene Islands, Madagascar and South Africa (Burbidge & Cummins 2007; Okal & Synolakis 2008).

During the era of analog instrumental seismicity (defined as 1900 to 1976), only five events are reported near the Java Trench with at least one magnitude greater than 7, none of them during the WWSSN years (1962–1975). Among them, this paper focuses principally on the earthquake of 1921 September 11, which Gutenberg & Richter (1954; hereafter GR) locate between the later tsunami earthquakes of 1994 and 2006, at 11°S, 111°E, with a magnitude $M_{PAS} = 7\frac{1}{2}$. This event is remarkable in that it was felt over a distance of 1500 km (Visser 1922), from Krui on Sumatra Island to Taliwang on Sumbawa (Fig. 1). However, its tsunami was moderate, reaching only a maximum amplitude of 10 cm on the published tide gauge at Cilacap (Fig. 2, reproduced from Solov'ev & Go (1984). Visser (1922) proposed an epicentre at 12.4°S, 110.8°E, based on a barycentric averaging of crude estimates given by the observatories of Batavia, Malabar and Riverview. He also transcribed a report from Riverview Observatory describing the Wiechert seismometer being flung off scale during the arrival of 20-s Rayleigh waves, as we were able to verify on the original record archived at Geoscience Australia in Canberra. Finally, Visser (1922) relates that the *S.S. Salawatti* reported being jolted by a 'seaquake' while sailing at 8.68°S and 112.37°E (star of David on Fig. 1), a phenomenon generally interpreted as resulting from the propagation of high-frequency

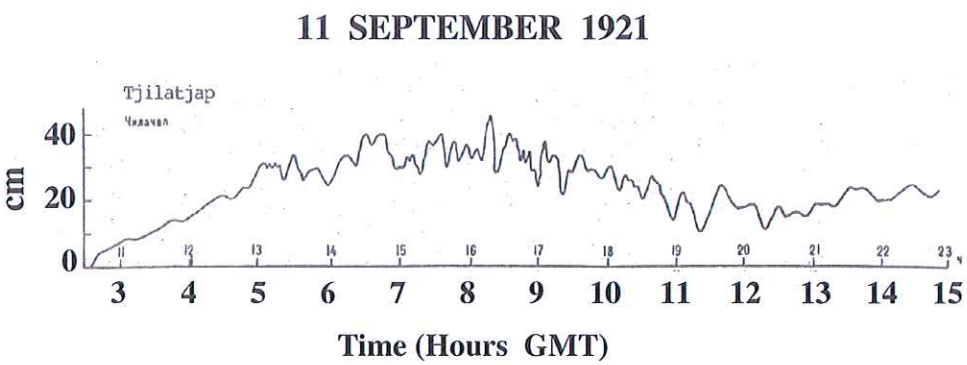

Figure 2. Maregram of the 1921 tsunami recorded at Cilacap (reproduced after Solov'ev & Go 1954). The smaller numbers above the horizontal axis give local time (GMT +8).

P waves refracted vertically into the oceanic column (Ambraseys 1985).

All this evidence suggests that the source of the 1921 earthquake was rich in high frequencies, and rules out that the event could be a 'tsunami earthquake' comparable to its neighbours in 1994 and 2006. This indicates that the regional character of the latter is not universal, even on a small geographic scale, a conclusion already hinted at in other subduction systems by Okal & Newman (2001). Rather, the 1921 event is evidence that large earthquakes do occur along the Java subduction zone without featuring the anomalously slow source spectrum of 'tsunami earthquakes', and that the seismicity of the Java Trench is clearly undersampled by the still young CMT catalogue.

However, the question of the exact nature of the 1921 earthquake in the local tectonic context remains open, as it could *a priori* involve a number of distinct geometries:

(i) a thrusting event expressing the relative motions of the two plates along the subduction interface, essentially the missing large interplate thrust event along this subducting segment;

(ii) an outboard normal faulting event reminiscent of the 1977 Sumba earthquake farther east;

(iii) an outer rise intraplate thrusting earthquake, in the geometry outlined by Chen & Forsyth (1978); or

(iv) an intraplate earthquake inside the Wadati-Benioff zone, presumably at an intermediate depth ($h \geq 70$ km), in a geometry possibly reminiscent of the 2006 Tonga or 2009 Padang, Sumatra earthquakes.

In favour of Scenarios (ii) or (iii) would be the preliminary location south of the Java Trench; in favour of (iv) would be the very large felt area, characteristic of intraplate, deeper events featuring higher stress drops (e.g. Chillan, 1939 January 25; Padang, 2009 September 30), and the moderate amplitude of the tsunami.

In addition to the 1921 event, we examine more briefly the earthquakes of 1937 September 27 ($M_{\rm PAS} = 7.2$) and 1943 July 23 ($M_{\rm PAS} = 8.1$). Regarding the event of 1916 September 11, listed by GR at 9°S, 113°E, $h = 100$ km ($M_{\rm PAS} = 7\frac{1}{4}$), it is not mentioned in the International Seismological Summery (ISS), and Gutenberg's notepads (Goodstein *et al.* 1980) list arrivals at only four stations, preventing any attempt at meaningful relocation. Finally, the earthquake of 1903 February 27, listed by GR at 8°S, 106°E ($M_{\rm PAS} = 8.1$), predates even B. Gutenberg's compiled notepads, and thus cannot be formally relocated. Based on fragmentary isoseismals, and the absence of a reported tsunami, Newcomb & McCann (1987) have argued that it is not an interplate thrust event, but rather an intraplate earthquake, either in westernmost Java or easternmost Sumatra.

2 RELOCATIONS

2.1 The 1921 earthquake

We relocated the 1921 earthquake using arrival times published by the ISS and the iterative interactive method of Wysession *et al.* (1991), which includes a Monte Carlo algorithm consisting of injecting Gaussian noise into the data set. For an event in the early 1920s, we use a standard deviation $\sigma_G = 10$ s. The solution uses 20 *P* and 1 *S* times and converges to 10.81°S, 111.45°E (large star on Fig. 1), with a root-mean-squares residual of only 4.7 s. This location is only 30 km south of the trench, with our Monte Carlo ellipse intersecting it. The hypocentral depth was fixed at 10 km, as it could not be resolved by the inversion. Relocations at other constrained depths show a weak increase of rms residual with depth, the epicentre remaining inside the Monte Carlo ellipse (Figs 1 and 3a).

As shown in Fig. 1, our relocated epicentre is 97 km northwest of the original ISS location (11.5°S, 112°E) and only 53 km northeast of GR's (11°S, 111°E). Most intriguing is Engdahl & Villaseñor's (2002) relocation as part of their Centennial Catalog (13.095°S, 110.077°E), 295 km southwest of our preferred epicentre, in an area with no known modern seismicity, as defined by centroids of the Global CMT catalogue with moments greater than 3×10^{24} dyn cm (Dziewonski *et al.* 1983 and subsequent updates), shown as small symbols on Fig. 1; note however that this location may be an artifact of a poor choice of initial epicentre (E.R. Engdahl, personal communication, 2011). Newcomb & McCann's (1987) solution (11.35°S, 110.76°E) also falls inside our confidence ellipse, 96 km southwest of our epicentre. We also inverted the arrival times used by GR to obtain their published estimate, as listed in B. Gutenberg's original notepads (Goodstein *et al.* 1980). This data set of 13 times converges on 11.17°S, 111.11°E, only 55 km from our epicentre, with a confidence ellipse largely overlapping ours. Incidentally, this location agrees perfectly with GR's estimate (being only 22 km away, and taking into account GR's rounding up their locations to the nearest half-degree); this illustrates the remarkable precision achieved by these authors using only pencil and paper.

Visser (1922) compiles eight widely felt aftershocks in the 80 days following the main event. None them is listed in the ISS, and thus they could not be relocated.

The conclusion of our relocation efforts is that the 1921 earthquake took place in the immediate vicinity of the trench; at this point, it could represent an interplate event on the uppermost part of the subduction interface (at the northeastern extremity of the confidence ellipse), or it could be an outer rise earthquake, similar at least in location to the 1977 Sumba event, if placed farther south

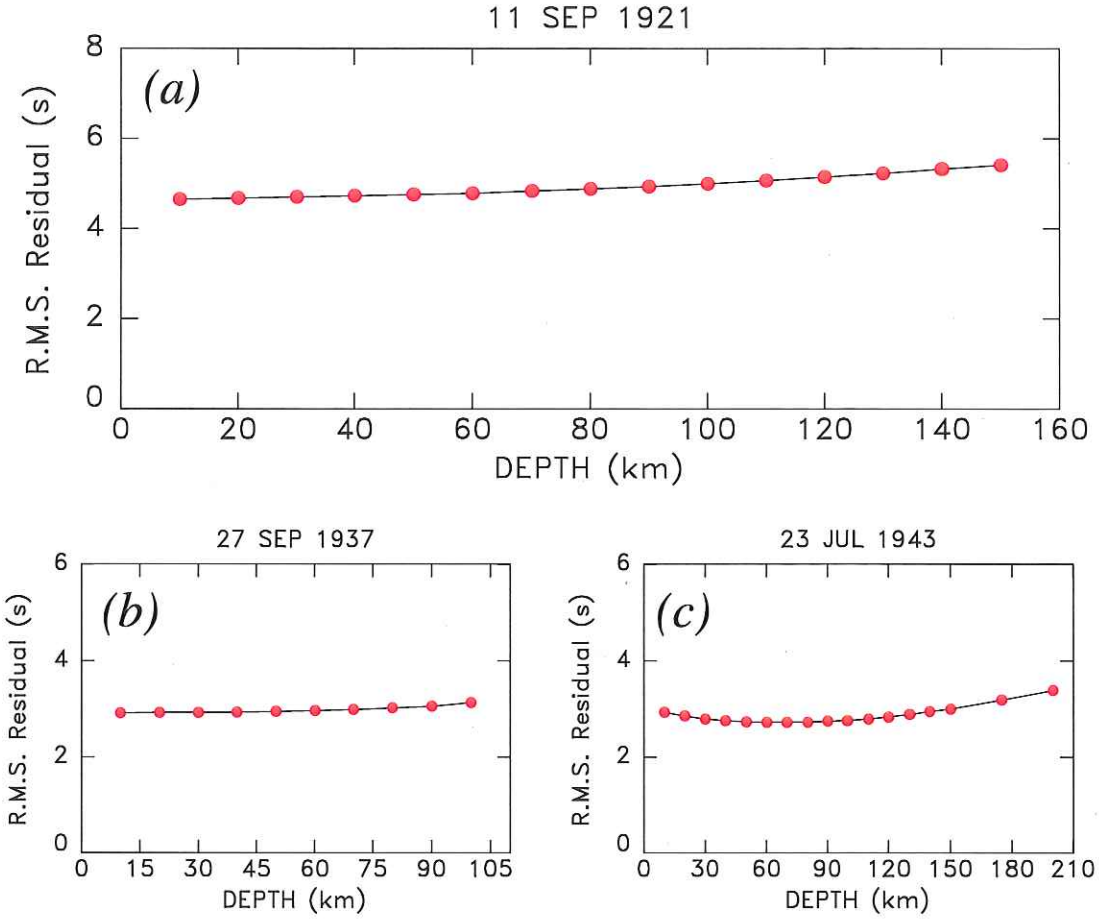

Figure 3. Root-means-square residuals of constrained-depth relocations of the 1921 (a), 1937 (b) and 1943 (c) events, as a function of the imposed depth. This figure illustrates the general lack of depth resolution of the available data sets.

inside the ellipse. We can rule out an intermediate depth event ($h \geq$ 70 km; scenario (iv) above), since our Monte Carlo ellipse remains at least 70 km from the relevant section of the Wadati-Benioff zone, as defined by Global CMT solutions deeper than 70 km, shown as the small triangles on Fig. 1.

2.2 Other shocks

We relocated the 1937 shock to 8.84°S, 110.71°E, only 18 km from the ISS location but 80 km northwest of GR's solution (9.5°S; 111°E). Our epicentre agrees well with modern solutions published by Newcomb & McCann (1987) (8.88°S, 110.65°E) and Engdahl & Villaseñor (2002) (9.02°S, 110.80°E), which fall within our small confidence ellipse ($\sigma_G = 6$ s). Unfortunately, the data set has no depth resolution (Fig. 3b), and even though the epicentre falls in the vicinity of the plate interface, the source could be *a priori* at the contact, above, or below it. We note that the larger ($m_b \geq 5$), well-located modern events in the immediate vicinity of the epicentre have depths between 50 and 90 km, and that the ISS gives an estimate at 65 km.

For the 1943 event, a floating depth relocation is possible, converging on 8.52°S, 109.90°, at $h = 52$ km (Fig. 1). This depth is in reasonable agreement with that proposed by the ISS (65 km), and used in Engdahl & Villaseñor's (2002) solution (8.55°S, 109.76°E). However, Fig. 3(c) shows that the available data set has only poor depth resolution; the interpretation of *sS-S* on the EW (*SH*) record at Wellington suggests a depth of 75 km. This would be compatible with the relocation of the 1943 event 150 km north of trench, identifying it as an intraplate earthquake in the slab, of which many modern, if smaller, examples are documented in its vicinity and shown as small triangles on Fig. 1.

3 FOCAL MECHANISMS AND MOMENTS

3.1 The 1921 earthquake

For the purpose of constraining the focal mechanism of the 1921 earthquake, we used a number of historical records, listed on Table 1. Original copies were scanned or photographed at archive centres or from the microfilm collections compiled in the 1980s under the auspices of IASPEI and the World Data Center A (Glover & Meyers 1987).

3.1.1 Body-wave constraints

Despite the scant azimuthal coverage of the available stations, we were able to read the following first motion information: impulsive kataseismic arrivals (corresponding to downwards vertical first motion) at Batavia, Riverview and Cape Town (*P*), and anaseismic

Table 1. Seismic records used in this study.

Station		Distance (°)	Azimuth (°)	Instrument type	Components used	Phases used
Code	Name					
API	Apia, western Samoa	74.8	101.5	Wiechert	EW	P
BAT	Batavia (Jakarta), Indonesia	6.5	314.5	Wiechert	NS, EW	P
CTO	Cape Town, South Africa	86.5	236.2	Milne-Shaw	EW	P, SKS, S
DBN	De Bilt, the Netherlands	108.5	321.3	Golitsyn	NS, EW	P_{diff}, R_1, G_1
GTT	Göttingen, Germany	105.6	320.5	Wiechert	NS	P_{diff}, G_1
PAR	Paris St. Maur	110.6	318.0	Golitsyn, Wiechert	Z, NS	P_{diff}, G_1
RIV	Riverview, NSW, Australia	42.9	128.7	Wiechert	NS	P, G_1
STR	Strasbourg, France	107.1	317.5	Wiechert	EW	P_{diff}
TOK	Hongo (Tokyo), Japan	60.6	26.4	Omori	NS	P, R_1

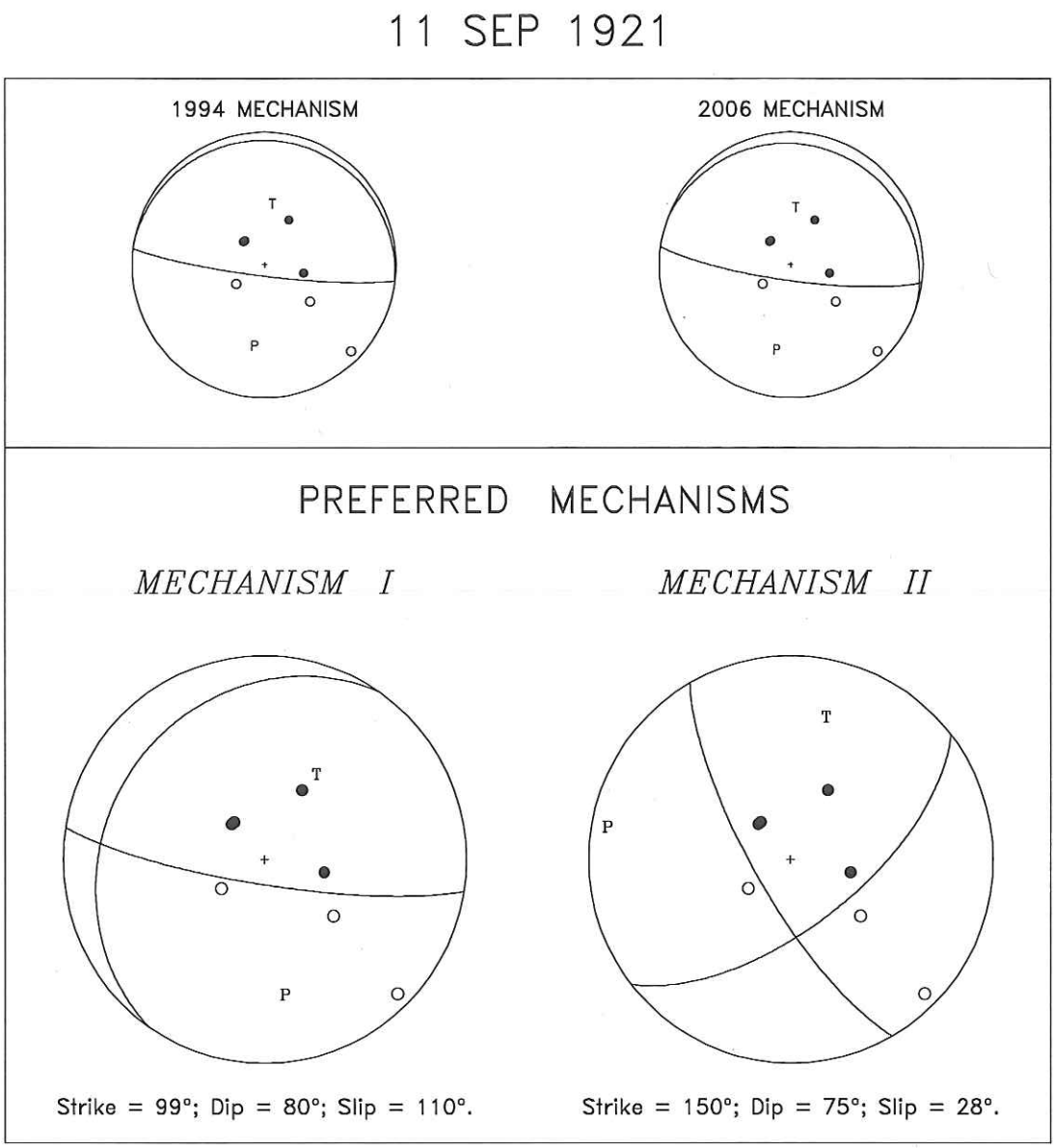

Figure 4. Focal mechanism of the 1921 event. Top: stereographic plots of first motion arrivals in the geometry of the 1994 and 2006 tsunami earthquake mechanisms. Bottom: the two classes of possible focal mechanism, as determined by P wave first motions. Solid dots and shaded areas are anaseismic arrivals, open ones kataseismic.

arrivals at Hongo and Apia (P) and De Bilt and Strasbourg ($Pdiff$).

While these P-wave polarities are insufficient to fully resolve the focal mechanism, they strongly constrain it. In particular, Fig. 4 shows that they are compatible with the mechanisms of the nearby 1994 and 2006 tsunami earthquakes. However, the large impulsive P wave at Batavia (Fig. 5) suggests a component of strike-slip on the steeply dipping plane (or alternatively, a significantly

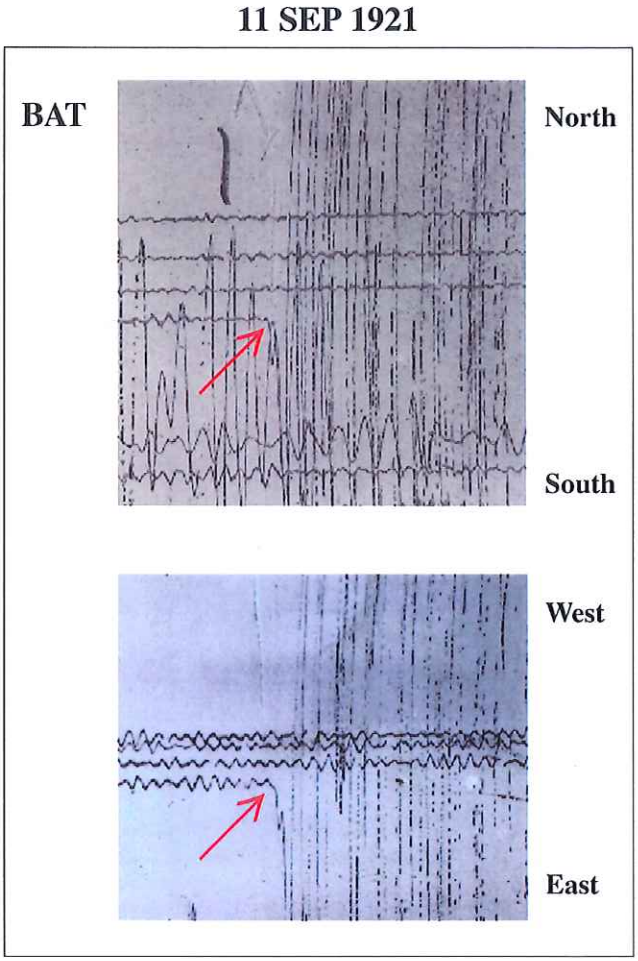

Figure 5. Close-up of the *P*-wave recordings of the 1921 earthquake on the Wiechert instrument at Batavia (Jakarta). Note the strongly impulsive kataseismic arrival to the southeast. The frames are 160 s long.

rotated strike for the shallow-dipping one). Fig. 4 shows a preferred mechanism (I) with $\phi = 99°; \delta = 80°; \lambda = 110°$. The *P*-wave data set would also be compatible with the alternate mechanism (II) $\phi = 150°; \delta = 75°; \lambda = 28°$, which is predominantly strike-slip. Mechanism 1 would be expected from a type (i) scenario (albeit with some obliquity) occurring in the northeastern corner of the Monte Carlo ellipse, while Mechanism II may represent a type (ii) or (iii) scenario taking place in its southern portion. Fig. 6 locates these two possible mechanisms relative to a cross-section of modern local seismicity, as relocated by Engdahl & Villaseñor (2002).

Additional constraints can be obtained from *S* waves. The EW record at Cape Town (the only component available; back-azimuth $\beta = 101°$), shown on Fig. 7(a), features a clear westwards *S* arrival, preceded by an *SKS* of opposite polarity, a classical result in this range of distances ($\Delta = 86°$). This observation cannot discriminate between the two mechanisms which both predict a westwards *S* arrival ($R^{S(\mathrm{EW})} = -0.27$ for I; -0.45 for II). However, the EW record at Apia (again, the only available component; $\beta = 262°$) shows a reasonably energetic *S*/*SKS* group (Fig. 7b), well predicted by the strike-slip solution II ($R^{S(\mathrm{EW})} = 0.31$; $R^{SKS} = 0.19$ at the source), while the thrusting mechanism I would predict vanishing amplitudes ($R^{S(EW)} = -0.03$; $R^{SKS} = 0.06$ at the source). These results tend to favour a Type II solution, although they remain more qualitative and tentative than those derived from first-motion *P*-wave polarities.

In conclusion, available body-wave constraints narrow down the possible focal geometry of the 1921 event to two classes of mechanisms: a thrusting mechanism on a shallow-dipping plane generally consistent with the subduction interface, albeit with some component of strike-slip (I); or a strike-slip mechanism with a slight component of thrust (II). Notwithstanding these difficulties, a major result from body-wave constraints is that the earthquake features a component of thrust faulting, and thus that it cannot be an outer rise normal faulting event comparable to the 1977 Sumba one. This rules out Scenario (ii) described in the Introduction.

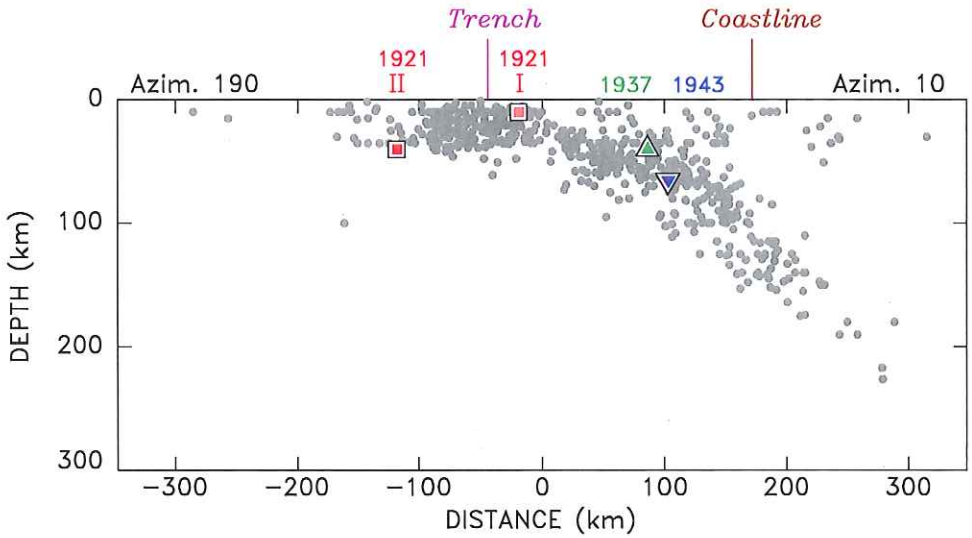

Figure 6. Cross-section of local seismicity with preferred hypocentral locations for the earthquakes of 1921 (square), 1937 (triangle) and 1943 (inverted triangle). The data set used in background is Engdahl & Villaseñor's (2002) between longitudes 108 and 114°E. For reference, the locations of the trench (at 111.8°E) and of the coastline (at 110°E) are shown. For the 1921 event, the two possible locations under Mechanisms I and II are shown.

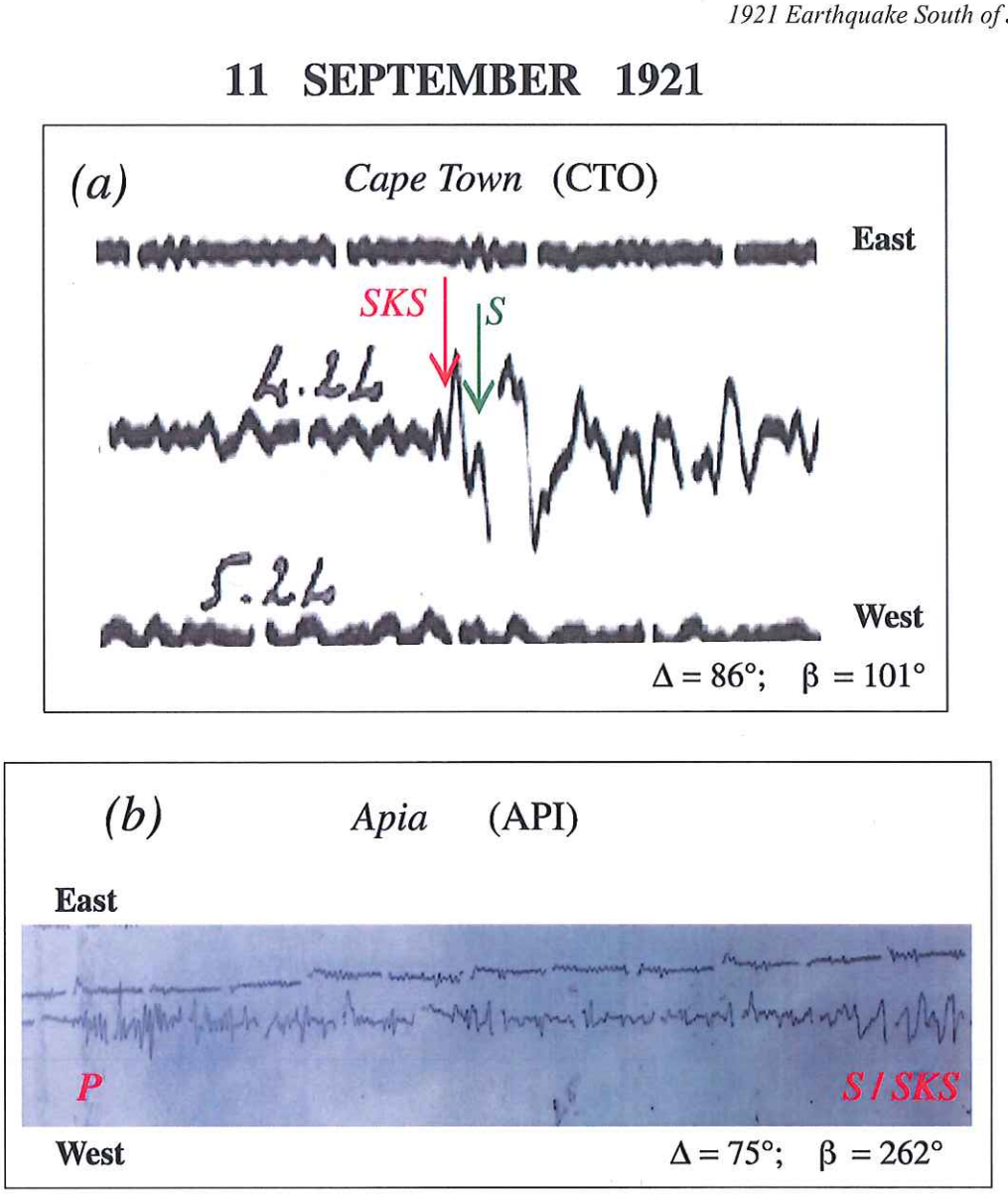

Figure 7. (a) Close-up of the *SKS/S* arrival of the 1921 event on the EW Milne-Shaw seismometer at Cape Town. (b) East–west component of the Wiechert record at Apia. The vertical scale of both seismograms has been exaggerated by a factor of 2. Minute marks shown as breaks on both records.

3.1.2 *Mantle waves*

We used first-order passages of Love waves (G_1) at Riverview, De Bilt and Göttingen, and of Rayleigh waves (R_1) at De Bilt and Hongo (Tokyo). The records were hand-digitized and equalized to a sampling $\delta t = 1$ s. Spectral amplitudes were then obtained in the mantle frequency range $4 \leq f \leq 12$ mHz, using the mantle magnitude formalism of Okal & Talandier (1989).

Because of poor azimuthal sampling, the PDFM inversion algorithm (Okal & Reymond 2003) could not converge. Rather, we consider the two classes of solutions suggested by the body-wave studies, and for each of them, compute magnitudes M_c corrected for focal mechanism (Okal & Talandier 1989). The latter are a direct expression of the seismic moment M_0 (in dyn cm) at the relevant frequencies:

$$\log_{10} M_0 = M_c + 20 \qquad (1)$$

On Fig. 8, we plot the resulting values of M_c as a function of frequency for the various records involved.

For the thrusting mechanism (Type I), the average value of M_c is 8.11 ± 0.40. Regarding the R_1 record on the NS Omori instrument at Hongo (E.R.I., Tokyo University), we use the constants listed by Kawasumi (1949), including a period of 53 s, which is remarkably long for that era, but essentially comparable to that listed by McComb & West (1931) for what is probably the same instrument. The resulting M_c values at Hongo exceed the 1-σ interval by 0.3 units (a factor of 2 on the moment). If we exclude these outlying values from the data set, the average becomes $M_c = 7.92 \pm 0.23$. We note however a trend towards an increase of moment with growing period, suggesting a static value in excess of 10^{28} dyn cm for this mechanism.

For the Type II (strike-slip) mechanism, Fig. 8 shows again that the Hongo values are 0.3 units larger than the 1-σ interval. The average values, including the Hongo data, are $M_c = 7.68 \pm 0.40$,

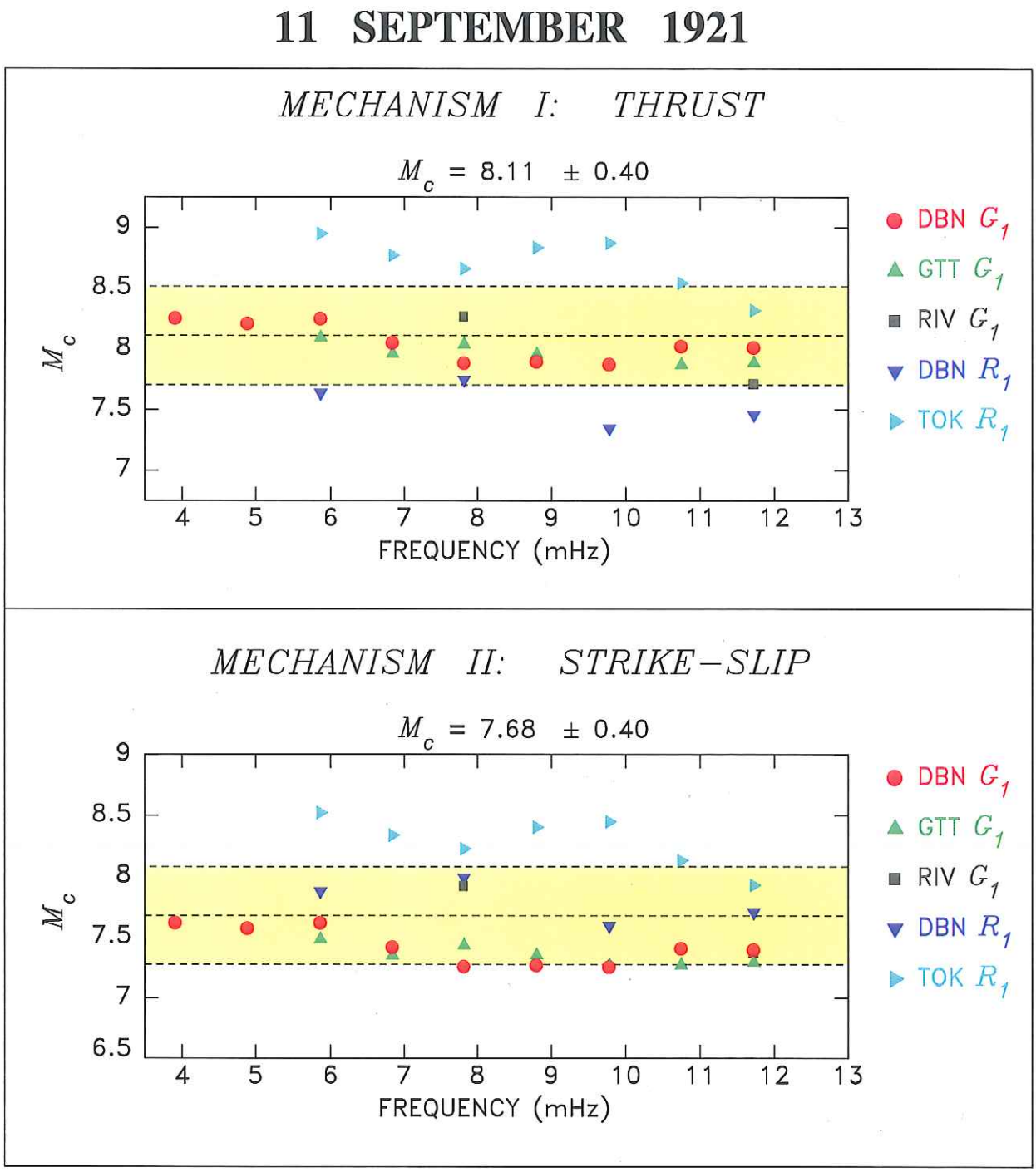

Figure 8. Mantle magnitude analysis of low-frequency surface waves from the 1921 event, under Mechanisms I (top) and II (bottom). For each mechanism, the values of M_c, the mantle magnitude corrected for focal mechanism (Okal & Talandier 1989), are plotted against frequency. The central dashed line and shaded area are the average value and 1-σ confidence interval, respectively.

corresponding to $M_0 = 4.8 \times 10^{27}$ dyn cm, within a multiplicative or divisive factor of 2.5. In the absence of the Tokyo R_1 record, this figure becomes $M_c = 7.49 \pm 0.22$.

In conclusion, mantle waves cannot discriminate between Type-I (thrust) and Type-II (strike-slip) mechanisms. The moment required by the latter is generally smaller, approximately by a factor of 2, which simply reflects the general properties of surface wave excitation at shallow depths.

3.2 The 1937 event

In the case of the 1937 event, we read kataseismic P wave first motions at Apia, Riverview, Batavia, Hongo, Tucson, Pasadena and De Bilt (selected examples shown on Fig. 9), complemented by kataseismic reports in the ISS at six more stations (Hong Kong, Ksara, Beograd, Toyooka, Weston and La Paz). A lone anaseismic ISS report at Zo-se is obviously incompatible with the rest of the

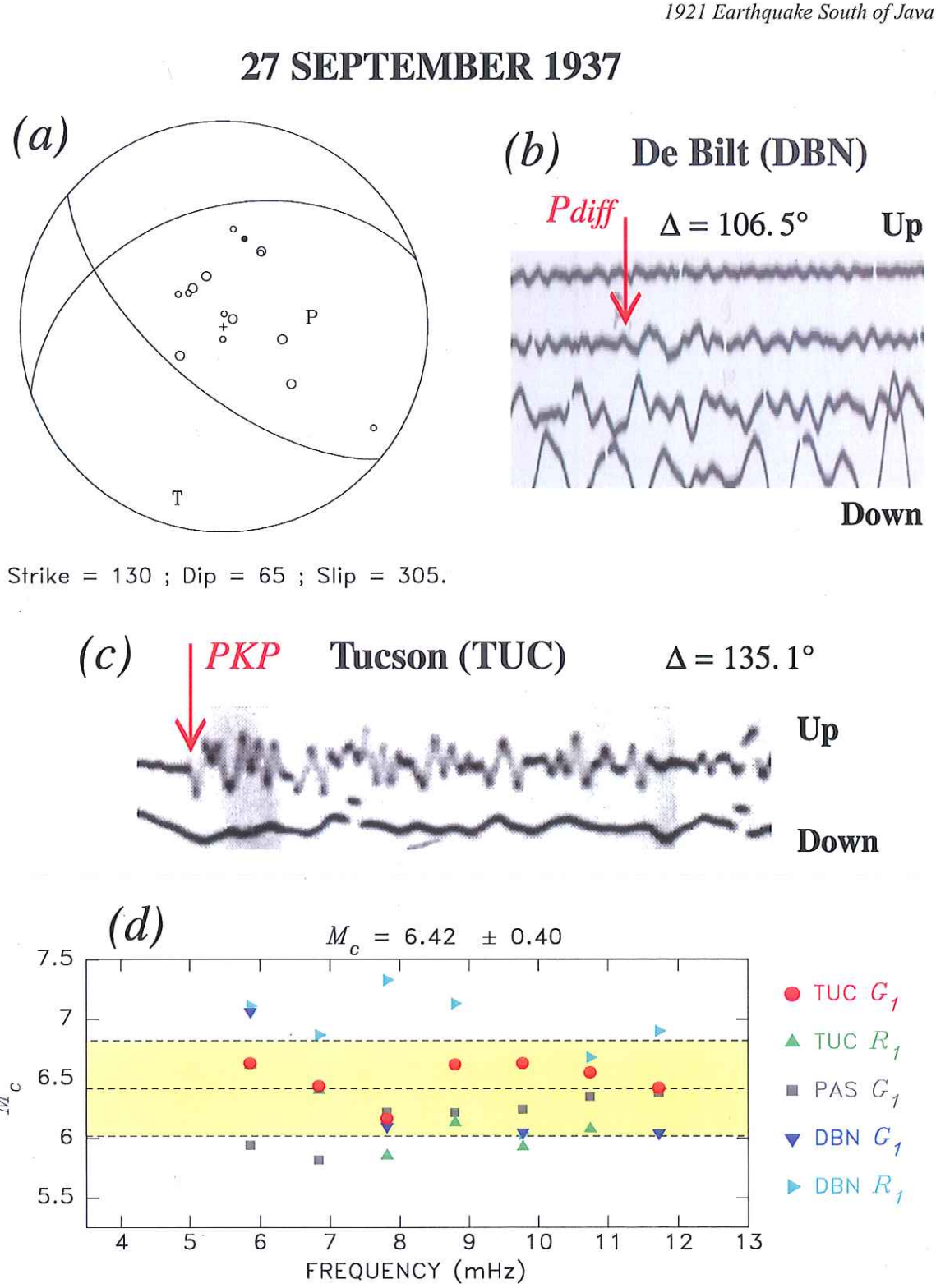

Figure 9. Focal mechanism and moment of the 1937 event. (a) Preferred focal solution based on polarities of first arrivals (large symbols read in this study; small ones reported by the ISS; open symbols and quadrants: kataseismic; closed symbol (Zo-se, obviously erroneous) and shaded quadrants: anaseismic), and *S* wave constraints. (b) Close-up of first arrival at De Bilt (*Pdiff*). The vertical scale of the record has been exaggerated by a factor of 2. (c) Close-up of impulsive *PKP* arrival at Tucson. These two kataseismic arrivals rule out a thrusting mechanism and hence an interplate event. (d) Estimate of moment from spectral amplitudes of mantle waves, as on Fig. 8.

data set. This data set clearly establishes the predominantly normal faulting character of the event. The focal mechanism proposed on Fig. 9 ($\phi = 130°; \delta = 65°; \lambda = 305°$) is also compatible with *SKS* polarities at De Bilt (to west) and Cape Town (to west), and *S* polarities at Cape Town (to east and south), Riverview (to south), and Apia (to east).

Mantle waves were processed at Tucson and De Bilt (G_1 and R_1) and Pasadena (G_1 only). In the focal geometry determined above,

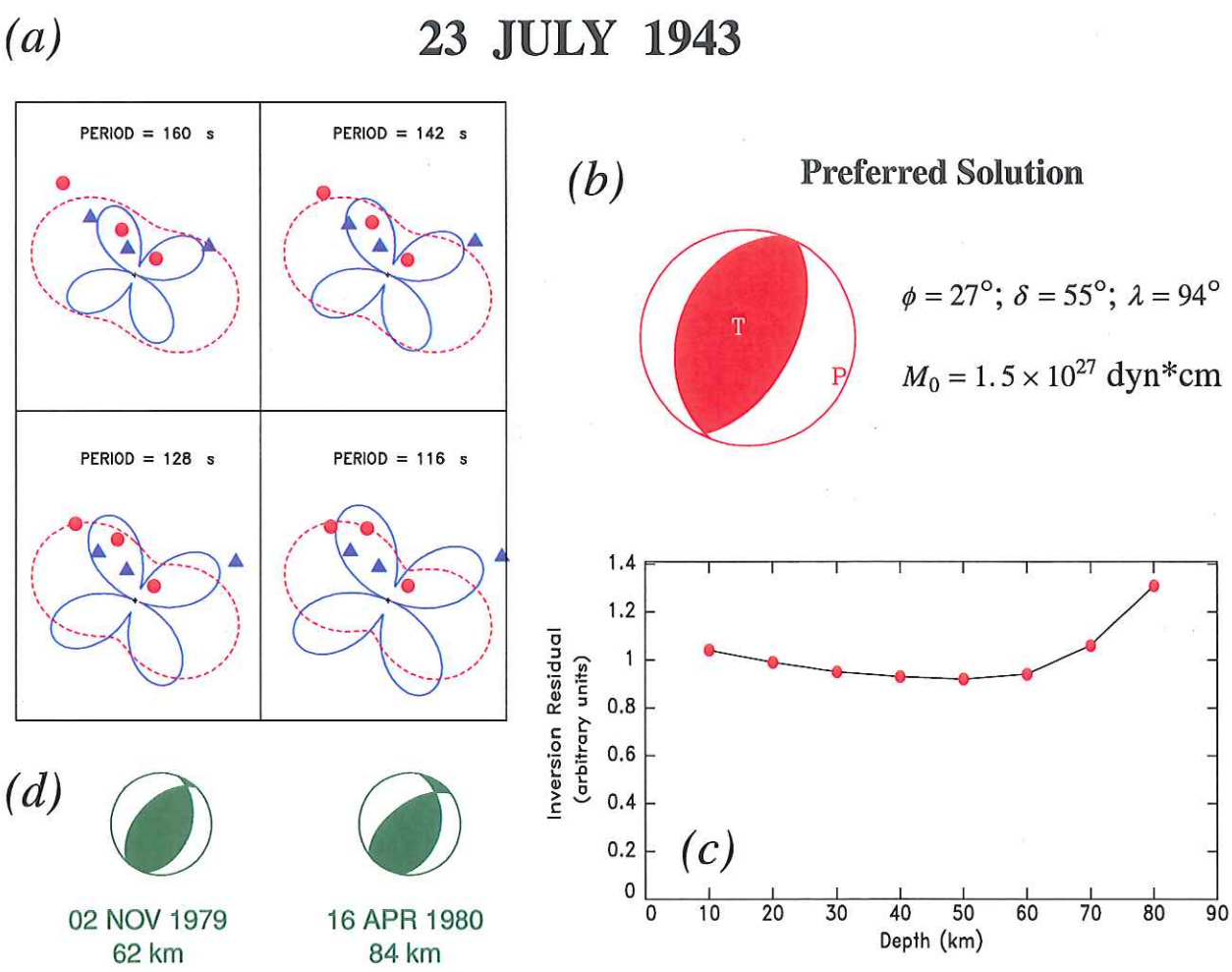

Figure 10. (a) Results of the PDFM inversion of the 1943 event. At each of the four selected periods, the observed spectral amplitudes (individual dots: Rayleigh; triangles: Love; all normalized to a distance of 90°) are compared to the theoretical radiation patterns (solid lines: Love; dashed: Rayleigh). Scales vary with period, but are common for a given period. (b) Final solution after lifting indeterminacies using body-wave constraints (see Fig. 11). (c) Inversion residual as a function of depth. Note the broad minimum from 40 to 60 km. (d) Modern events from the Java subduction system with comparable focal mechanisms and depths.

they lead to $M_c = 6.42 \pm 0.40$ or $M_0 = 2.6 \times 10^{26}$ dyn cm within a multiplicative or divisive factor of 2.5.

In conclusion, the 1937 earthquake cannot express slip on the slab interface, but rather is a normal faulting, probably intra-slab, event. Its relatively weak moment and probable depth explain the absence of a documented tsunami. Comparable solutions exist, albeit at a smaller size, in the modern record (1992 June 9; 1995 May 5).

3.3 The 1943 event

In the case of the 1943 earthquake, we successfully used the PDFM method (Reymond & Okal 2000) to invert a data set of three Rayleigh waves (De Bilt, Tucson and San Juan) and three Love waves (De Bilt, Honolulu and San Juan). Fig. 10 shows the preferred mechanism ($\phi = 27°; \delta = 55°; \lambda = 94°$). The 180° indeterminacies in slip and strike angles inherent in the method (Romanowicz & Suárez 1983; Reymond & Okal 2000) are easily lifted by the impulsive anaseismic arrivals at Melbourne (*P*), De Bilt (*Pdiff*) and Tucson and San Juan (*PKP*), and the strong *SH* (to north) arrival at Honolulu (see Fig. 11). This mechanism is also compatible with *S*, *sS* and *ScS*(*SH*) southwards arrivals at Wellington. Inversion residuals feature a broad minimum between 40 and 65 km depth. While the focal geometry is perfectly robust over that depth range, the inverted moment varies from 1.5 (at 40 km) to 2.2 (at 65 km) $\times 10^{27}$ dyn cm. It remains however significantly smaller than suggested by GR's assigned magnitude, $M_{\rm PAS} = 8.1$.

4 TSUNAMI SIMULATIONS

4.1 The 1921 event

In this section, we carry out a number of tsunami simulations in order to further discriminate between the possible source scenarios of the 1921 earthquake. For this purpose, we use the only known quantitative record of the 1921 tsunami, namely the tidal gauge record at Cilacap, reproduced on Fig. 2 from Solov'ev & Go (1984), with a zero-to-peak amplitude not exceeding 10 cm.

We then select four sources. In Model I-A, we consider a Type I mechanism (predominantly thrust faulting) rupturing the thrust interface in material featuring standard mechanical properties. In Model I-B, we consider the same source, but rupturing weaker material in a geometry reminiscent of Bilek & Lay's (1999) model; we are motivated in this respect by our relocation results, which allow an interplate rupture only in the northernmost part of our

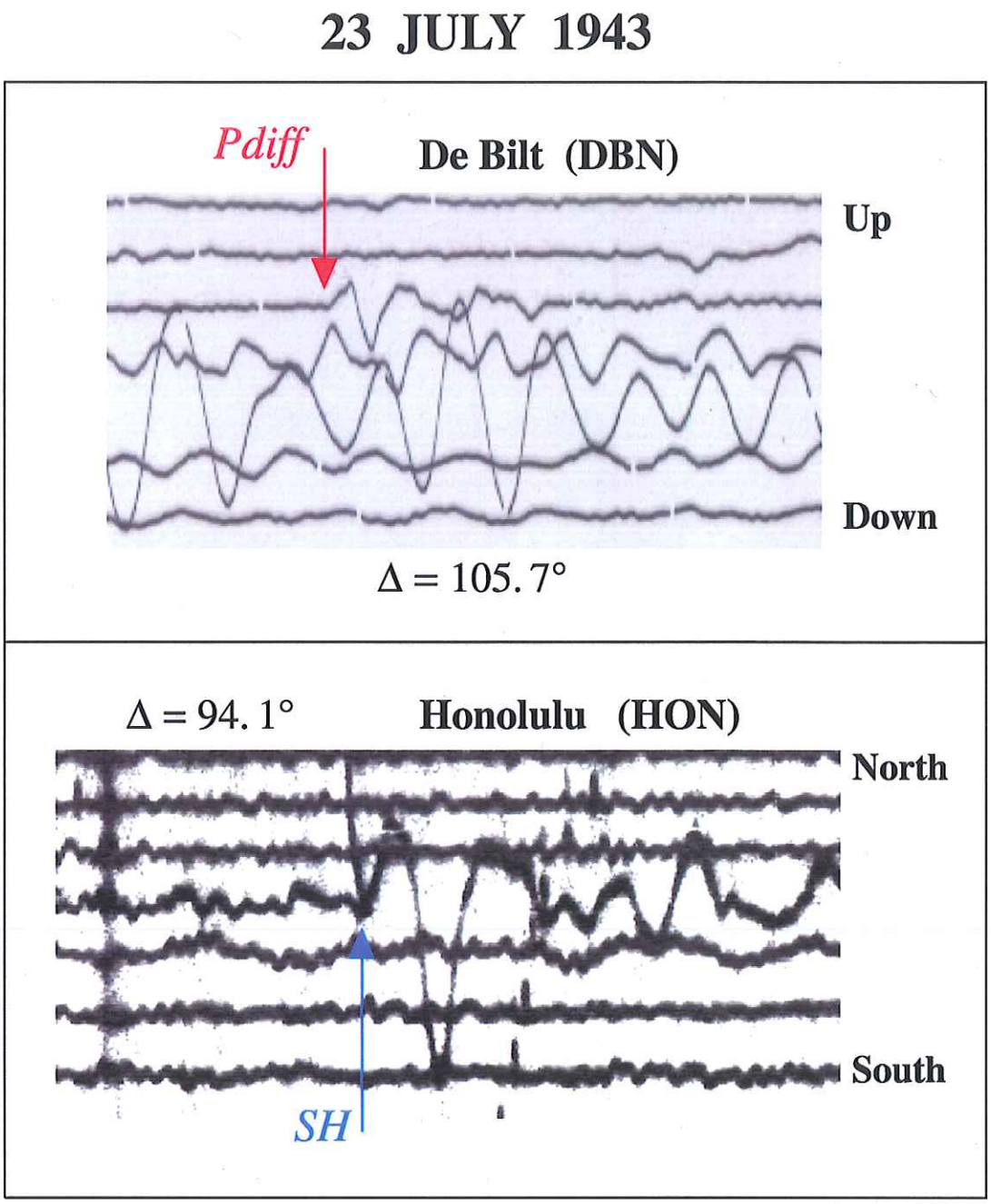

Figure 11. Close-up of body-wave polarities lifting the 180° strike and slip indeterminacies in the PDFM inversion results for the 1937 earthquake. Top: the *Pdiff* arrival on the vertical Golitsyn record at DBN requires a component of thrust. Bottom: the impulsive *SH* arrival to North on the Milne-Shaw instrument at Honolulu (back-azimuth $\beta = 263°$) favours the shallower dip to the WNW, and thus the strike of 27°.

confidence ellipse, i.e. along the uppermost part of the interplate contact, in the vicinity of the trench. In Model II-C, we consider a Type II mechanism (predominantly strike-slip) rupturing in standard material, the top of the fault being at 15 km. Finally, in Model II-D, we sink the source 15 km deeper into the plate. In Type-I models (A and B), the centroid of rupture is positioned at the northern extremity of our uncertainty ellipse, while in Type-II models (C and D), it is located in the outer rise. All relevant details of the four models are listed in Table 2.

For each of the four models considered, we use scaling laws (Geller 1976) to infer appropriate fault dimensions and obtain a field of surface static displacements in the epicentral area using Mansinha & Smylie's (1971) algorithm, which we then use as an initial condition for sea surface displacement in a numerical simulation using the MOST code (Titov & Synolakis 1998). The latter solves the non-linear equations of hydrodynamics under the shallow-water approximation, using a finite difference algorithm and the method of alternate steps; MOST has been extensively validated through benchmarking with laboratory and field data, per standard international protocols. All details can be found in Synolakis (2003).

In the absence of adequate small-scale bathymetry near the port of Cilacap, we use a bathymetric grid with a sampling of 0.1 degree, and we consider a virtual gauge located in deep water, 40 km southeast of Cilacap, at 8°S; 109.4°E, and identified by the diamond on Fig. 1. We start by simulating the 2006 tsunami, using the GlobalCMT geometry, and obtain a zero-to-peak amplitude of 77 cm at

Table 2. Source parameters used in tsunami simulations.

Source		Focal geometry			Centroid		Depth	Source parameters			Rigidity	Moment	Amplitude at
Mechanism type	Model	Strike ϕ(°)	Dip δ(°)	Rake λ(°)	Latitude (°S)	Longitude (°E)	(km)	Slip (m)	Length (km)	Width (km)	(10^{11} dyn cm^{-2})	(10^{27} dyn cm)	virtual gauge (cm)
Reference: 2006 Tsunami earthquake													
2006 JUL 17		290	10	102	9.25	107.41	10	6.0	110	40	1.9	5	77
1921 September 11													
I	A	215	22	27	10	112	10	3.3	111	56	5	10	22
I	B	215	22	27	10	112	10	6.6	150	66	1.9	10	66
I	C	150	75	28	11	111	15	4.0	72	30	6	5.2	14
II	**D**	**150**	**75**	**28**	**11**	**111**	**30**	**4.0**	**72**	**30**	**6**	**5.2**	**6**
1937 September 27													
1937	E	130	65	305	−8.84	110.71	10	0.9	35	17	5	0.3	5
1937	F	130	65	305	−8.84	110.71	65	0.85	35	17	6	0.3	1
1943 July 23													
1943	G	27	55	94	−8.52	109.90	40	1.2	60	30	7	1.5	2
1943	H	27	55	94	−8.52	109.90	65	1.4	67	34	7	2.2	1.5

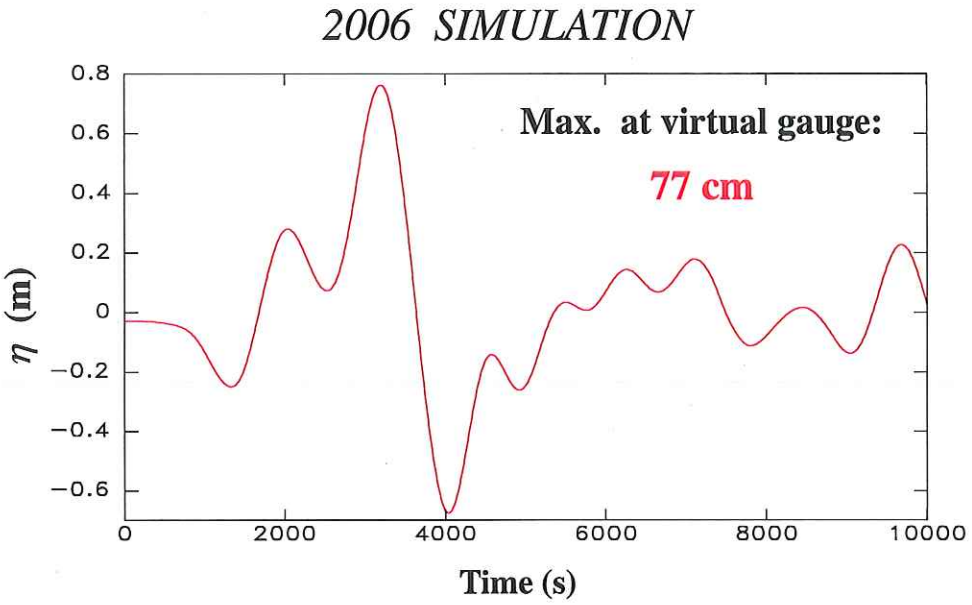

Figure 12. Simulation of the 2006 tsunami at the deep water virtual gauge located off Cilacap (diamond on Fig. 1). The comparison of the maximum amplitude (77 cm) with that recorded on the Cilacap maregraph (1.25 m) defines an empirical factor of ~1.6 between the virtual gauge and the maregraph.

the virtual gauge (Fig. 12). A comparison with the amplitude of 1.25 m actually recorded at Cilacap (Rahma Hanifa *et al.* 2008) defines an amplification factor of ~1.6 between the deep water virtual gauge and the tidal gauge at Cilacap (we assume that the latter was not moved between 1921 and 2006). Conversely, given the 1921 amplitude at Cilacap, we then seek a solution simulating a 6 cm (zero-to-peak) amplitude at the virtual gauge.

Fig. 13 shows that Type-I models (A and B) produce much larger amplitudes. In particular, Model I-B yields an amplitude comparable to, if somewhat smaller than, in 2006, despite a higher moment, reflecting the more oblique nature of the Type-I focal mechanism. While the strike-slip mechanism used in Model II-C produces a lower amplitude (14 cm), it is still too large (estimated 22 cm at Cilacap), and only Model II-D produces an amplitude of 6 cm at the virtual gauge. We conclude that the moderate tsunami documented on the tidal record at Cilacap can be successfully explained only by Model II-D, namely a mostly strike-slip solution, taking place in the bottom part of the bending lithosphere, as sketched on Fig. 6.

4.2 The 1937 and 1943 events

We also simulated the smaller events of 1937 and 1943 to verify that our models would not produce observable tsunamis. In the case of the 1937 shock, we consider a shallow source (10 km; Model E) and a deeper one (65 km; Model F), as suggested by the ISS, and more in line with the modern seismicity around the epicentre. The former gives an amplitude of 5 cm at the virtual gauge, suggesting 8 cm at Cilacap, which might have been observed, given the daylight occurrence of the event. The latter produces only 1 cm at the virtual gauge, or less than 2 cm in Cilacap, which would most likely have gone unnoticed both by the population, and on the tidal gauge record.

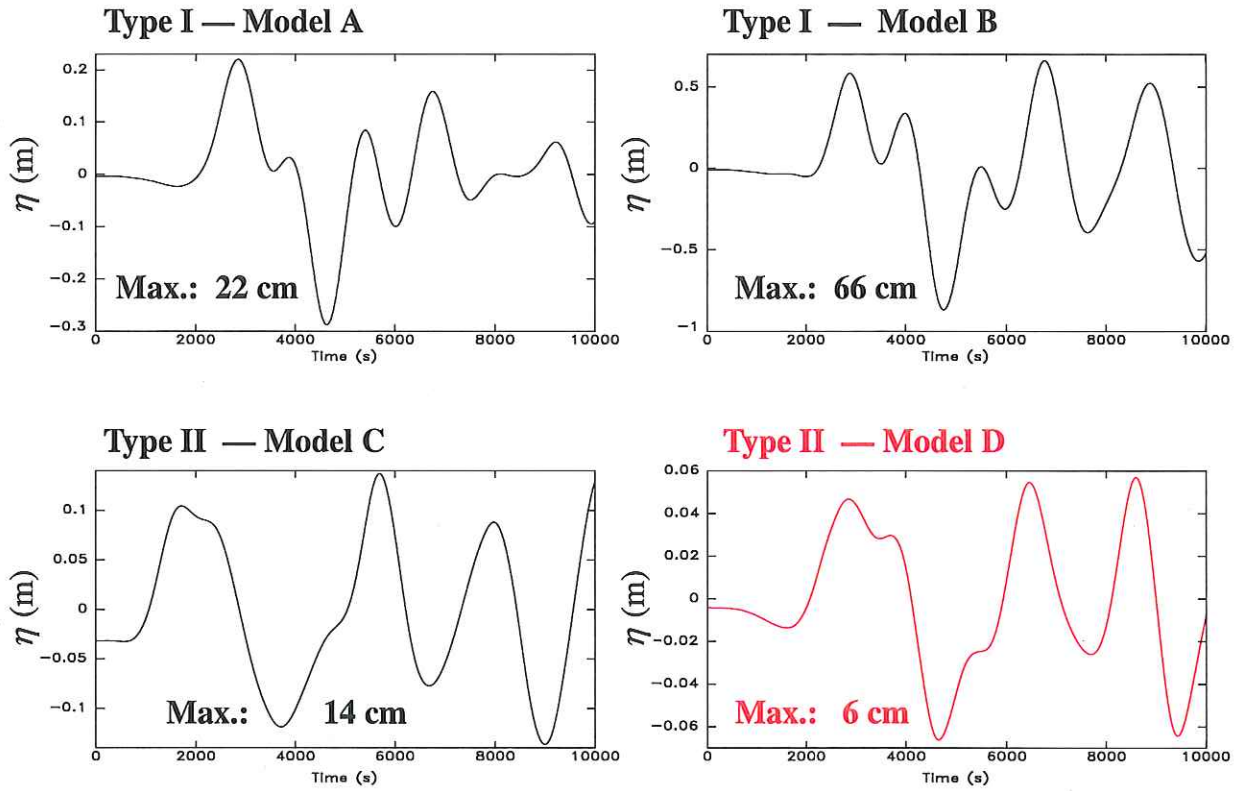

Figure 13. Tsunami simulations at the virtual gauge (diamond on Fig. 1) for the four source models of the 1921 earthquake listed in Table 2. Note that only Model D, featuring a deeper Type II (strike-slip) geometry, features a small amplitude compatible with the 10 cm observed at Cilacap (Fig. 2).

In the case of the decisively deeper 1943 shock, we use Model G at 40 km, and Model H at 65 km. They produce tsunamis with amplitudes of 2 and 1.5 cm, respectively, at the virtual gauge, suggesting amplitudes of at most 3 cm at Cilacap. It is doubtful that such amplitudes would have been noticed, especially given their night time occurrence (22:30 solar time at 109°E).

We conclude that our preferred solutions are generally compatible with the absence of reported tsunamis in 1937 and 1943.

5 DISCUSSION AND CONCLUSION

Based on the above observations and studies, we can reject the following models for the 1921 earthquake.

(1) It cannot be an intra-slab earthquake comparable to the Padang event of 2009 September 30 (McCloskey *et al.* 2010). Based on a deep focus ($h \geq 70$ km) and a higher stress drop, this scenario ((iv) in Section 1) could have explained the exceptionally wide felt area, and the mediocre tsunami. But our relocation excludes this possibility since our Monte Carlo ellipse (even its northernmost part) remains at least 70 km south of the position of the Wadati-Benioff zone at the relevant depths, as mapped by modern seismicity.

(2) It cannot be a normal faulting outer rise earthquake comparable to the 1977 Sumba event (Sce nario (ii) in Section 1), since its focal mechanism has a strong component of thrust.

(3) It cannot be a conventional interplate thrust event, under Scenario (i) of Section 1. A Type-I focal mechanism would generate a much larger tsunami than recorded at Cilacap, especially so since our relocation would require the event to occur along the uppermost part of the subduction interface in a geometry likely to result in a 'tsunami earthquake' under the models of Tanioka *et al.* (1997) or Bilek & Lay (1999), which is clearly not the case of the 1921 earthquake.

The only remaining possibility is Scenario (iii) of Section 1, i.e. an outer rise event locating south of the trench, in the centre of our confidence ellipse, with a Type-II, predominantly strike-slip focal mechanism. We have shown that this reconciles the *S* wave observations at Apia, and if the source is deep enough in the plate, it can explain the mediocre tsunami recorded at Cilacap. Note that the *T* axis of the mechanism shown on Fig. 4 (plunge 30°; azimuth 14°) expresses tension perpendicular to the trench, and is only rotated (26 ± 3)° (2 ± 7° in azimuth) from that of bending earthquakes documented in the area, albeit at a much lower moment level (e.g. 2009 September 7; 2.2×10^{25} dyn cm).

In conclusion, of the three historical (1900–1976) earthquakes reported along the Java trench with at least one magnitude greater than 7 (1921, 1937, 1943), none can be an interplate thrust event. Thus, the largest known earthquakes of this type at the Java Trench, including historical events, are the tsunami earthquakes of 1994 and 2006, whose moments remain relatively small by subduction zone standards. While this situation is reminiscent of those at the Nicaragua and Hikurangi trenches and in the northern Peru segment of the Nazca Trench, it does not necessarily mean that mega-thrust earthquakes are excluded from the Java Trench.

To verify this possibility, we present on Fig. 14 a frequency-moment regression of the data set of all GlobalCMT solutions (1977– 2011 November) with a thrusting mechanism in the

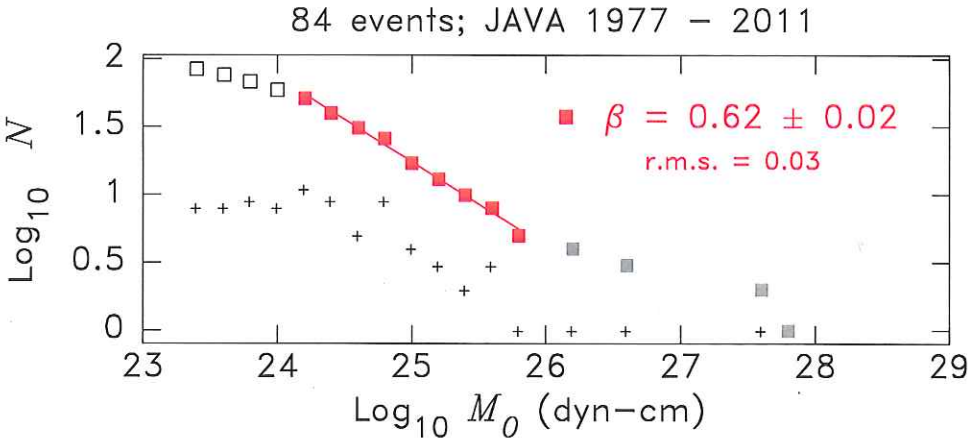

Figure 14. Frequency-moment statistics for GlobalCMT thrust fault solutions at the Java Trench. The + signs represent the populations in each bin, the larger symbols are cumulative populations. The regression (shown by the solid line) is performed on the data set of solid symbols. The open ones to the left correspond to an incomplete population, and the half-tone symbols to the right correspond to bins with only one earthquake. Both are excluded from the regression.

province. We define the latter as having a P-axis inclined less than 40° on the horizontal, a T-axis dipping more than 50°, and an N-axis dipping less than 20°. We regress the data set only between moments of 10^{24} and 6×10^{25} dyn cm, an arguably small window, but for which the data set is both complete and reasonably sampled, none of the bins (0.2 logarithmic units in moment) showing less than 2 events. Note that, while all of these earthquakes have thrust mechanisms, they may not all be actual *interplate* events. The resulting regression

$$\log_{10} N = 16.7 - 0.62 \log_{10} M_0 \quad (2)$$

features a β-value (Molnar 1979) close to the theoretical value of 2/3 (Rundle 1989). When extrapolated beyond the regressed segment, eq. (2) predicts 4 (exactly 3.8) events beyond 10^{26} dyn cm, where indeed 4 were observed (including the two tsunami earthquakes). Conversely, and assuming that the distribution expressed by eq. (2) extends to larger sources, it would predict an event of moment 10^{28} dyn cm every 160 years, and a megathrust event ($M_0 \geq 10^{29}$ dyn cm) every 670 years. Our study shows that the former is missing from the era of historical seismicity (post-1900), but it could have occurred in the previous century, even though Newcomb & McCann (1987) have argued, based on isoseismal data and on the lack of known tsunami reports, that the known large earthquakes of 1867 and 1875 may have taken place on land. As for the latter, the historical record, as compiled for example by Solov'ev & Go (1984), does not go back reliably beyond 1750 A.D. In summary, our study fails to identify thrusting events larger than the two tsunami earthquakes of 1994 and 2006, but the available seismic record is too short to formally preclude their rare occurrence. In particular, there is no evidence to suggest that the scaling law expressed by eq. (2) should not be applicable at higher moments. This result is similar to Okal *et al.*'s (2012) recent conclusions in the Mariana-Bonin subduction zone, and would generally support the concept that megathrust events might occur in all subduction systems (McCaffrey 2007; Stein & Okal 2007).

Finally, we note that the scenario unraveled here for the 1921 earthquake—a relatively deep strike-slip earthquake in the outer rise of the Australian plate—is generally comparable to that of the recent, much larger, twin events of 2012 April 11 off the coast of northern Sumatra ($M_0 = 9$ and 4×10^{28} dyn cm, respectively), in a region where, only a few months before their occurrence, Choy & Kirby (2011) had described four smaller events ($M_0 \leq 2.7 \times 10^{26}$ dyn cm) of similar geometry. With the exception of the more distant second 2012 event, these earthquakes are located 55 to 135 km seaward of the Sumatra trench, and their depths, as determined by the NEIC, range from 11 to 35 km (note that GlobalCMT centroid depths for the 2012 events reach 40 and 54 km, respectively); the first 2012 event, and the four shocks studied by Choy & Kirby (2011) feature high stress drops. All six focal mechanisms are characterized by T axes oriented within a few degrees of the direction of convergence between the plates (as determined by the mechanisms of the large 2004 Aceh, 2005 Nias and 2007 Bengkulu events). All these properties are reproduced in our preferred, Type II, mechanism for the 1921 earthquake, whose T axis strikes N14°E, only 6° away from the direction of dip of the 2006 solution. This T-axis geometry is also shared with the earthquake of 1942 June 14 recently identified by Okal *et al.* (2012) in the southern Marianas, and more generally with a family of smaller shocks originally observed by Chen & Forsyth (1978).

Another doublet of large strike-slip earthquakes ($M_0 = 7.5$ and 7.9×10^{27} dyn cm, respectively) occurred on 2000 June 4 and 18 off southern Sumatra, the first one being an intra-slab event under the fore-arc, and the second one an intraplate shock in the Wharton Basin, 1100 km to the SSW (Abercrombie *et al.* 2003). Both of these shocks were complex, composite events, but the first one also features a tensional axis in the direction of convergence at the trench. Neither of them generated a tsunami observable in Sumatra.

Christensen & Ruff (1983), and later Dmowska *et al.* (1988), have suggested that the stresses released by outer-rise earthquakes may be time-controlled within the earthquake cycle, with a compressional regime preceding the interplate thrust events, and a tensional one following them, while tensional events should occur downdip from the main thrust zone during the later part of the seismic cycle. The large 2012 earthquakes off northern Sumatra would generally fit this model in relation to the 2004 Aceh and 2005 Nias megathrust events, as would, further south, the intraslab earthquake of 2000 June 4 relative to the 2007 Bengkulu earthquake. We note however, that the 2009 intraslab Padang earthquake, featured a mechanism very similar to that of the first 2000 shock (rotated only 14° in Kagan's (1991) formalism), but took place *after* the 2007 Bengkulu interplate thrust event (McCloskey *et al.* 2010). Similarly, Choy & Kirby's (2011) smaller earthquakes occurred both before (1995) and after (2005–2007) the Aceh megathrust. Finally, both the 2000 and 2012 sequences occurred in the context of the diffuse boundary between the Indian and Australian plates (Wiens *et al.* 1985; Gordon *et al.* 1990), which gives rise to an additional field of

stresses unrelated to the simple model of a conventional subduction zone, as used by Dmowska *et al.* (1988). In this framework, it would seem highly speculative to venture any interpretation of the 1921 earthquake in terms of the timing of a putative megathrust cycle at the Java subduction zone.

ACKNOWLEDGMENTS

I am grateful to Brian Ferris (Lower Hutt), Ian Saunders (Pretoria), Bernard Dost (De Bilt), Tiar Prasetya (Jakarta), Geneviève Patau (St. Maur), Steve Kirby and James Dewey (USGS) for access to historical seismological archives. Bob Engdahl cast a refreshing perspective on the problem of secondary minima during earthquake relocations. George Choy kindly shared the characteristics of the events described in Choy & Kirby (2011) prior to publication. Some figures were prepared using the GMT software (Wessel & Smith 1991). Data collection was partially supported by the USGS Tsunami Scenario Project.

REFERENCES

Abercrombie, R.E., Antolik, M. & Ekström, G., 2003. The June 2000 M_w = 7.9 earthquakes south of Sumatra: deformation in the India-Australia plate, *J. geophys. Res.*, **108**(Bl), doi:10.1029/2001JB000674.

Ambraseys, N.N., 1985. A damaging seaquake, *J. Earthq. Eng. Struct. Dynam.*, **13,** 421–424.

Bilek, S.L. & Lay, T., 1999. Rigidity variations with depth along interplate megathrust faults in sub duction zones, *Nature,* **400,** 443–446.

Burbidge, D. & Cummins, P.R., 2007. Assessing the threat to Western Australia from tsunamis generated by earthquakes along the Sunda Arc, *Natural Hazards,* **43,** 319–331.

Chen, T. & Forsyth, D.W., 1978. A detailed study of two earthquakes seaward of the Tonga Trench: implications for the mechanical behavior of the oceanic lithosphere, *J. geophys. Res.*, **83,** 4995–5003.

Choy, G.L. & Kirby, S.H., 2011. Stress conditions at the subduction inferred from differential earthquake magnitudes, *Am. geophys. Un. Fall Meeting 2011,* Abstract S54B-01.

Christensen, D.H. & Ruff, L.J., 1983. Outer-rise earthquakes and seismic coupling, *Geophys. Res. Lett.*, **10,** 697–700.

Dmowska, R., Rice, J.R., Lovison, L.C. & Josell, D., 1988. Stress transfer and seismic phenomena in coupled subduction zones during the earthquake cycle, *J. geophys. Res.*, **93,** 7869–7884.

Dziewonski, A.M., Friedman, A., Giardini, D. & Woodhouse, J.H., 1983. Global seismicity of 1982: centroid-moment tensor solutions for 308 earthquakes, *Phys. Earth planet. Inter.*, **33,** 76–90.

Engdahl, E.R. & Villaseñor, A., 2002. Global seismicity: 1900-1999, in *International Handbook of Earthquake and Engineering Seismology,* pp. 665–690, eds Lee, W.H.K., Kanamori, H., Jennings, P.C. & Kisslinger, C., Academic Press, Boston, MA.

Fritz, H.M. *et al.*, 2007. Extreme runup from the 17 July 2006 Java tsunami, *Geophys. Res. Lett.*, **34,** L12602, doi:10.1029/2007GL029404.

Fukao, Y., 1979. Tsunami earthquakes and subduction processes near deep-sea trenches, *J. geophys. Res.*, **84,** 2303–2314.

Geller, R.J., 1976. Scaling relations for earthquake source parameters and magnitudes, *Bull. seism. Soc. Am.*, **66,** 1501–1523.

Glover, D.P. & Meyers, H., 1987. Historical seismogram filming project: current status, in *Historical Seismograms and Earthquakes of the World,* pp. 373–379, eds Lee, W.H.K., Meyers, H. & Shimazaki, K., Academic Press, San Diego, CA.

Goodstein, J.R., Kanamori, H. & Lee, W.H.K., 1980. Seismology microfiche publications from the Caltech archives, *Bull. seism. Soc. Am.,* **70,** 657–658.

Gordon, R.G., DeMets, D.C. & Argus, D.F., 1990. Kinematic constraints on distributed lithospheric deformation in the equatorial Indian Ocean from present motion between Australian and Indian plates, *Tectonics,* **9,** 409–422.

Gutenberg, B. & Richter, C.F., 1954. *Seismicity of the Earth and Associated Phenomena,* Princeton Univ. Press, Princeton, NJ, 310pp.

Kagan, Y.Y., 1991. 3-D rotation of double-couple earthquake sources, *Geophys. J. Int.*, **106,** 709–716.

Kanamori, H., 1972. Mechanism of tsunami earthquakes, *Phys. Earth planet. Inter,* **6,** 346–359.

Kawasumi, H., 1949. Seismology in Japan, 1939–1947, *Bull. seism. Soc. Am.*, **39,** 157–167.

Lay, T. & Bilek, S.L., 2007. Anomalous earthquake ruptures at shallow depths on subduction zone megathrusts, in *The Seismogenic Zone of Subduction Thrust Faults,* pp. 476–511, eds Dixon, T. & Moore, C., Columbia Univ. Press, New York, NY.

Mansinha, L. & Smylie, D.E., 1971. The displacement fields of inclined faults, *Bull. seism. Soc. Am.*, **61,** 1433–1440.

McCaffrey, R., 2007. The next great earthquake, *Science,* **315,** 1675–1676.

McCloskey, J., Lange, D., Tilmann, F., Nalbant, S.S., Bell, A.F., Natawidjaja, D.H. & Rietbrock, A., 2010. The September 2009 Padang earthquake, *Nature Geosci.*, **3,** 70–71.

McComb, H.E. & West, C.J., 1931. List of seismological stations of the world, *Bulletin of the National Research Council,* Vol. **82,** p. 118. National Academy of Sciences, Washington, D.C.

Molnar, P., 1979. Earthquake recurrence intervals and plate tectonics, *Bull. seism. Soc. Am.*, **69,** 115–133.

Mueller, R.D., Roest, W.R., Royer, J.-Y., Gahagan, L.M. & Sclater, J.G., 1997. Digital isochrons of the world's ocean floor, *J. geophys. Res.*, **102,** 3211–3214.

Newcomb, K.R. & McCann, W.R., 1987. Seismic history and seismotectonics of the Sunda Arc, *J. geophys. Res.*, **92,** 421–439.

Newman, A.V., Hayes, G., Wei, Y. & Convers, J., 2011. The 25 October 2010 Mentawai tsunami earthquake, from real-time discriminants, fault rupture, and tsunami excitation, *Geophys. Res. Lett.*, **38**(5), L05302, doi:10.1029/2010GL046498.

Okal, E.A. & Borrero, J.C., 2011. The 'tsunami earthquake' of 22 June 1932 in Manzanillo, Mexico: seismological study and tsunami simulations, *Geophys. J. Int.*, **187,** 1443–1459.

Okal, E.A. & Newman, A.V., 2001. Tsunami earthquakes: the quest for a regional signal, *Phys. Earth planet. Inter.*, **124,** 45–70.

Okal, E.A. & Reymond, D., 2003. The mechanism of the great Banda Sea earthquake of 01 February 1938: applying the method of preliminary determination of focal mechanism to a historical event, *Earth planet. Sci. Letts.*, **216,** 1–15.

Okal, E.A. & Synolakis, C.E., 2008. Far-field tsunami hazard from megathrust earthquakes in the Indian Ocean, *Geophys. J. Int.*, **172,** 995–1015.

Okal, E.A. & Talandier, J., 1989. M_m: a variable period mantle magnitude, *J. geophys. Res.*, **94,** 4169–4193.

Okal, E.A., Reymond, D. & Hongsresawat, S., 2012. Large, pre-digital earthquakes of the Bonin-Mariana subduction zone, 1930–1974, *Tectonophysics,* submitted.

Polet, J. & Kanamori, H., 2000. Shallow subduction zone earthquakes and their tsunamigenic potential, *Geophys. J. Int.*, **142,** 684–702.

Rahma Hanifa, N., Sagiya, T., Kimata, F., Abidin, H.Z. & Meilano, I., 2008. Numerical modelling of the Java 2006 tsunami earthquake, constrained with coseismic displacement from GPS observation, tide gauge data, and tsunami run-up height, *Proc. Seismol. Soc. Japan 2008 Fall Mtg.*, Tsukuba (abstract).

Reymond, D. & Okal, E.A., 2000. Preliminary determination of focal mechanisms from the inversion of spectral amplitudes of mantle waves, *Phys. Earth planet. Inter,* **121,** 249–271.

Romanowicz, B.A. & Suárez, G., 1983. An improved method to obtain the moment tensor depth of earthquakes from the amplitude spectrum of Rayleigh waves, *Bull. seism. Soc. Am.*, **73,** 1513–1526.

Ruff, L.J. & Kanamori, H., 1980. Seismicity and the subduction process, *Phys. Earth planet. Inter.*, **23,** 240–252.

Rundle, J.B., 1989. Derivation of the complete Gutenberg-Richter magnitude frequency relation using the principle of scale invariance, *J. geophys. Res.*, **94,** 12 337–12 342.

Sella, G.F., Dixon, T.H. & Mao, A., 2002. REVEL: a model for recent plate velocities from space geodesy, *J. geophys. Res.*, **107**(B4), doi:10.1029/2000JB000033.

Solov'ev, S.L. & Go, Ch. N., 1984. Catalogue of tsunamis on the Western shore of the Pacific Ocean, *Can. Transl. Fish. Aquat. Sci.*, **5077,** 439pp.

Stein, S. & Okal, E.A., 2007. Ultra-long period seismic study of the December 2004 Indian Ocean earthquake and implications for regional tectonics and the subduction process, *Bull. seism. Soc. Am.*, **97,** S279–S295.

Synolakis, C.E., 2003. Tsunami and seiche, in *Earthquake Engineering Handbook,* pp. 9_1–9_90, eds Chen, W.-F. & Scawthron, C., CRC Press, Boca Raton, FL.

Tanioka, Y. & Satake, K., 1996. Fault parameters of the 1896 Sanriku tsunami earthquake estimated from tsunami numerical modeling, *Geophys. Res. Lett.*, **23,** 1549–1552.

Tanioka, Y., Ruff, L.J. & Satake, K., 1997. What controls the lateral variation of large earthquake occurrence along the Japan trench?, *Island Arc,* **6,** 261–266.

Titov, V.V. & Synolakis, C.E., 1998. Numerical modeling of tidal wave runup, *J. Wtrwy Port Coast. Engng,* **B124,** 157–171.

Tsuji, Y. *et al.*, 1995. Field survey of the East Java earthquake and tsunami of June 3, 1994, *Pure appl. Geophys.*, **144,** 839–854.

Visser, S.W., 1922. Vulkanische verschijnselen en aardbevingen in den Oost Indische archipel waargenomen gedurende jaar 1921, *Natuurkunding Tijdschrift voor Nederlandisch Indië,* **82,** 232–235.

Wessel, P. & Smith, W.H.F., 1991. Free software helps map and display data, *EOS, Trans. Am. geophys. Un.,* **72,** 441, 445–446.

Wiens, D.A. *et al.*, 1985. A diffuse plate boundary model for Indian Ocean tectonics, *Geophys. Res. Lett.*, **12,** 429–432.

Wysession, M.E., Okal, E.A. & Miller, K.L., 1991. Intraplate seismicity of the Pacific Basin, 1913–1988, *Pure appl. Geophys.*, **135,** 261–359.